



## **Substituent Effects in 3,3' Bipyrazole Derivatives. X-ray Crystal Structures, Molecular Properties and DFT Analysis**

Ibrahim Bouabdallah, Tarik Harit, Mahmoud Rahal, Driss Eddike, Monique Tillard,  
Fouad Malek

### **► To cite this version:**

Ibrahim Bouabdallah, Tarik Harit, Mahmoud Rahal, Driss Eddike, Monique Tillard, et al.. Substituent Effects in 3,3' Bipyrazole Derivatives. X-ray Crystal Structures, Molecular Properties and DFT Analysis. Acta Chimica Slovenica, 2021, 68 (3), pp.718-727. <10.17344/acsi.2021.6756>. <hal-03357395>

**HAL Id: hal-03357395**

**<https://hal.science/hal-03357395v1>**

Submitted on 28 Sep 2021

**HAL** is a multi-disciplinary open access archive for the deposit and dissemination of scientific research documents, whether they are published or not. The documents may come from teaching and research institutions in France or abroad, or from public or private research centers.

L'archive ouverte pluridisciplinaire **HAL**, est destinée au dépôt et à la diffusion de documents scientifiques de niveau recherche, publiés ou non, émanant des établissements d'enseignement et de recherche français ou étrangers, des laboratoires publics ou privés.



HAL Authorization

Scientific paper

# Substituent Effects in 3,3' Bipyrazole Derivatives. X-ray Crystal Structures, Molecular Properties and DFT Analysis

Ibrahim Bouabdallah,<sup>1</sup> Tarik Harit,<sup>1,\*</sup> Mahmoud Rahal,<sup>2</sup> Fouad Malek,<sup>1</sup> Monique Tillard<sup>3</sup> and Driss Eddike<sup>1</sup>

<sup>1</sup> Laboratory of Applied Chemistry and Environment, Faculty of Sciences, Mohammed First University Bd Mohamed VI, BP: 717, Oujda 60000, Morocco.

<sup>2</sup> Laboratoire de Chimie Physique, Faculté des Sciences, Université Chouaib Doukkali, BP 20, 24000, El Jadida, Morocco

<sup>3</sup> ICGM, Univ Montpellier, CNRS, ENSCM, Montpellier, France

\* Corresponding author: E-mail: tarikharit@gmail.com; t.harit@ump.ac.ma.  
Tel.: +212 536 500 601, Fax: +212 536 500 603

Received: 02-17-2021

## Abstract

The single crystal X-ray structure of new 1,1'-bis(2-nitrophenyl)-5,5'-diisopropyl-3,3'-bipyrazole, **1**, is triclinic  $P\bar{1}$ ,  $a = 7.7113(8)$ ,  $b = 12.3926(14)$ ,  $c = 12.9886(12)$  Å,  $\alpha = 92.008(8)$ ,  $\beta = 102.251(8)$ ,  $\gamma = 99.655(9)^\circ$ . The structural arrangement is compared to that of 5,5'-diisopropyl-3,3'-bipyrazole, **5**, whose single crystal structure is found tetragonal  $I4_1/a$ ,  $a = b = 11.684(1)$ ,  $c = 19.158(1)$  Å. The comparison is also extended to the structures previously determined for 1,1'-bis(2-nitrophenyl)-5,5'-propyl-3,3'-bipyrazole, **2**, 1,1'-bis(4-nitrophenyl)-5,5'-diisopropyl-3,3'-bipyrazole, **3**, and 1,1'-bis(benzyl)-5,5'-diisopropyl-3,3'-bipyrazole, **4**. Density Functional Theory (DFT) calculations are used to investigate the molecular geometries and to determine the global reactivity parameters. The geometry of isolated molecules and the molecular arrangements in the solid state are analyzed according to the nature of the groups connected to the bipyrazole core.

**Keywords:** Crystal structure; bipyrazole; DFT; substituent; reactivity indices.

## 1. Introduction

The C,C-linked bipyrazole derivatives have taken much interest in several fields.<sup>1</sup> Indeed, they have proven to be useful as potential anti-inflammatory,<sup>2</sup> cytotoxic,<sup>3</sup> anti-fungal,<sup>4</sup> extracting<sup>5</sup> and inhibitor corrosion<sup>6</sup> agents. These compounds also found applications in the synthesis of polymer materials.<sup>7</sup> Some authors have reported that bipyrazole compounds are active components and in particular, they are able to capture active oxygen and free radicals *in-vivo*.<sup>8</sup> Then, bipyrazoles are used as agents for preventing or treating various diseases induced by active oxygen.<sup>8</sup> Moreover, they have found a more unexpected application in the rocket industry as novel oxygen-rich energetic materials.<sup>9</sup>

It has been reported that the position and the nature of substituents on the pyrazole ring considerably affect

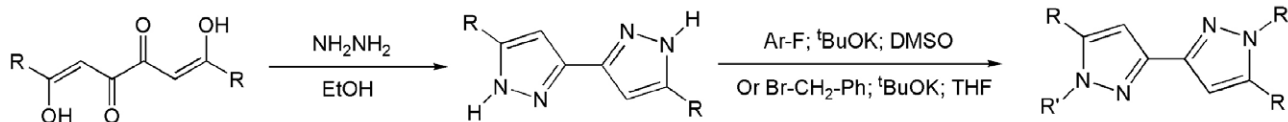
their biological activities as well as their catalytic and complexing properties.<sup>3-5,10,11</sup> However, and to the best of our knowledge, no study has attempted to describe their effects on the geometry of molecules and the structure of compounds.

This paper presents the single crystal structures of 1,1'-di(2-nitrophenyl)-5,5'-diisopropyl-3,3'-bipyrazole, **1**, and 5,5'-diisopropyl-3,3'-bipyrazole, **5**, analyzed comparatively with those of similar bipyrazole compounds. An analysis of the molecular geometry and the arrangement of molecules in crystals is carried out for five compounds differing by the nature of their R1 and R2 substituents. The molecules' geometry has been optimized using DFT calculations enabling an evaluation of the reactivity through quantum chemical reactivity descriptors.

## 2. Experimental and Computational Details

### 2.1. Synthesis of 1 and 5

The C,C-linked bipyrazole derivatives 1–5 were generally synthesized according to the literature method,<sup>12,13</sup> as represented in Scheme 1.



Scheme 1. General synthetic pathway to C,C-linked bipyrazoles 1–5

The compound **1** ( $C_{24}H_{24}N_6O_4$ ,  $M_r = 460.49$ ) was collected as a solid by filtration and oven-dried in vacuum. Yellow single crystals were obtained by recrystallization in ethanol. Compound **5** recrystallized from ethanol, has been synthesized by the condensation of hydrazine with 3,8-dihydroxy-2,9-dimethyl deca-3,7-diene-5,6-dione. The homogeneity of these compounds in their crystallized form was checked by spectroscopic methods (IR, NMR...) and found similar to those reported in our previous works.<sup>12,13</sup>

### 2.2. Data Collection and Refinement

A stereomicroscope equipped with a polarizing filter was used to select single crystals suitable for X-ray diffraction study. Experiments were carried out on Xcalibur CCD (Oxford Diffraction) four-circle diffractometer, using the Mo K $\alpha$  radiation and the CrysAlis software.<sup>14</sup> A yellow platelet of **1** of dimensions  $0.06 \times 0.15 \times 0.21$  mm was chosen to record the diffracted intensities at room temperature within the complete sphere. It displayed the triclinic  $P\bar{1}$  symmetry with lattice parameters  $a = 7.713(3)$ ,  $b = 12.371(6)$ ,  $c = 12.986(5)$  Å,  $\alpha = 92.07(3)$ ,  $\beta = 102.36(4)$ ,  $\gamma = 99.54(4)^\circ$ . A colorless square bipyramid of **5** with dimensions  $0.17 \times 0.20 \times 0.30$  mm was used for data collection at  $-100^\circ\text{C}$ . It displayed the tetragonal  $I4_1/a$  symmetry with lattice parameters  $a = 11.685(1)$ ,  $c = 19.158(1)$  Å. The data sets, including symmetry equivalent and redundant reflections, were merged as unique reflection data sets for uses in structure solution with the program SHELXS97<sup>15</sup> and full-matrix least-squares refinements on  $F^2$  with the program SHELXL97.<sup>16</sup> The atomic positions and anisotropic displacement parameters were refined for all non-hydrogen atoms. The H atoms were treated as riding, following the HFIX/AFIX instructions, they were given an isotropic displacement parameter equal to  $-1.2$  times ( $-1.5$  for terminal  $-\text{CH}_3$ ) the Ueq of the parent C atom. The main crystallographic data for **1** and **5** are reported in Table 1, comparatively with those of the other bipyrazole derivatives 2–4. The corresponding CIF files are available at the Cam-

bridge crystallographic data center<sup>17</sup> and can be obtained free of charge with the CCDC numbers 1879242 (**1**) and 1877532 (**5**).

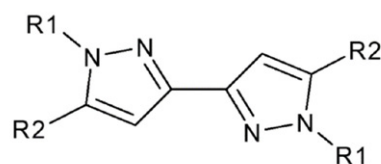
### 2.3. Computational Details

Geometries were optimized without any symmetry constraints at the DFT (density functional theory) level.

Calculations were performed using the tools implemented in the program Gaussian03W<sup>18</sup> with B3LYP functional and 6-31G(d,p) and 6-311++G(d,p) basis sets. The quantum mechanical code Dmol<sup>3</sup> was also used in full geometry optimization tasks by minimization of the total energy with B3LYP hybrid functional, effective core potentials and double numerical plus polarization DNP basis sets.<sup>19,20</sup> The GaussView 5.0.8<sup>21</sup> and Materials studio<sup>22</sup> interfaces were used to develop and visualize the molecular structures and their calculated properties.

## 3. Results and Discussion

The information that will be presented and discussed below concerns five molecules of bipyrazole derivatives, based on a 3,3'-bipyrazole core substituted at the 1,1' and 5,5' positions by different chemical R groups (Fig. 1).



- |  |   |
|--|---|
| 1 : R1 = o-NO <sub>2</sub> C <sub>6</sub> H <sub>4</sub> – | R2 = –CH(CH <sub>3</sub> ) <sub>2</sub>               |
| 2 : R1 = o-NO <sub>2</sub> C <sub>6</sub> H <sub>4</sub> – | R2 = –CH <sub>2</sub> CH <sub>2</sub> CH <sub>3</sub> |
| 3 : R1 = p-NO <sub>2</sub> C <sub>6</sub> H <sub>4</sub> – | R2 = –CH(CH <sub>3</sub> ) <sub>2</sub>               |
| 4 : R1 = –CH <sub>2</sub> C <sub>6</sub> H <sub>4</sub>    | R2 = –CH(CH <sub>3</sub> ) <sub>2</sub>               |
| 5 : R1 = –H  | R2 = –CH(CH <sub>3</sub> ) <sub>2</sub>               |

Fig. 1. Molecular structure of compounds considered in this work

All these molecules are centrosymmetric and their comparison deserves to be conducted to understand how the different functional groups act on their geometry, on their packing in solid state and thus on their chemical properties. The crystal structures of several compounds, the molecular geometries and the indices of global reactivity will be analyzed comparatively to evaluate these substituents effects. All the molecules considered in this work are formed with a 3,3'-bipyrazole core and bear R1 substit-

uent, hydrogen, nitro-phenyl or benzyl, attached to the N atom of the pyrazole ring at the 1,1' positions and R2 substituent, either linear propyl or isopropyl group, attached to the neighboring C atom at the 5,5' positions.

### 3. 1. Crystal Structure of 1

The structure displays the triclinic symmetry and is described in the  $P\bar{1}$  space group which is the most common for organic crystals. The unit cell of dimensions  $a = 7.7113(8)$ ,  $b = 12.3926(14)$ ,  $c = 12.9886(12)$  Å,  $\alpha = 92.008(8)$ ,  $\beta = 102.251(8)$ ,  $\gamma = 99.655(9)^\circ$  contains two molecules of 1,1'-(2-nitrophenyl)-5,5'-isopropyl bipyrazole (Fig. 2) in which phenyl rings are connected to the nitrogen atom of the 3,3'-bipyrazole core while the isopropyl group is attached to the neighboring carbon atom.

The calculated density of  $1.282 \text{ g}\cdot\text{cm}^{-3}$  is in line with the expectations for such a compound. The two molecules in the lattice of **1** are chemically equivalent but, as can be seen with the atom labels indicated in Fig. 2, they are crystallographically independent. Each molecule is placed on an inversion center located in the middle of the C1C1 and C21C21 bonds. The crystal structure of **1** brings a proof that the isolated regio-isomer adopts the form 1,1'-bis(2-nitrophenyl)-5,5'-diisopropyl-3,3'-bipyrazole which well agrees with the results of our previous works.<sup>12,13,23,24</sup>

### 3. 2. Crystal Structure of 5

The structure of 5,5'-di-isopropyl-1,1'-H-3,3'-bipyrazole was solved from low-temperature diffraction data.

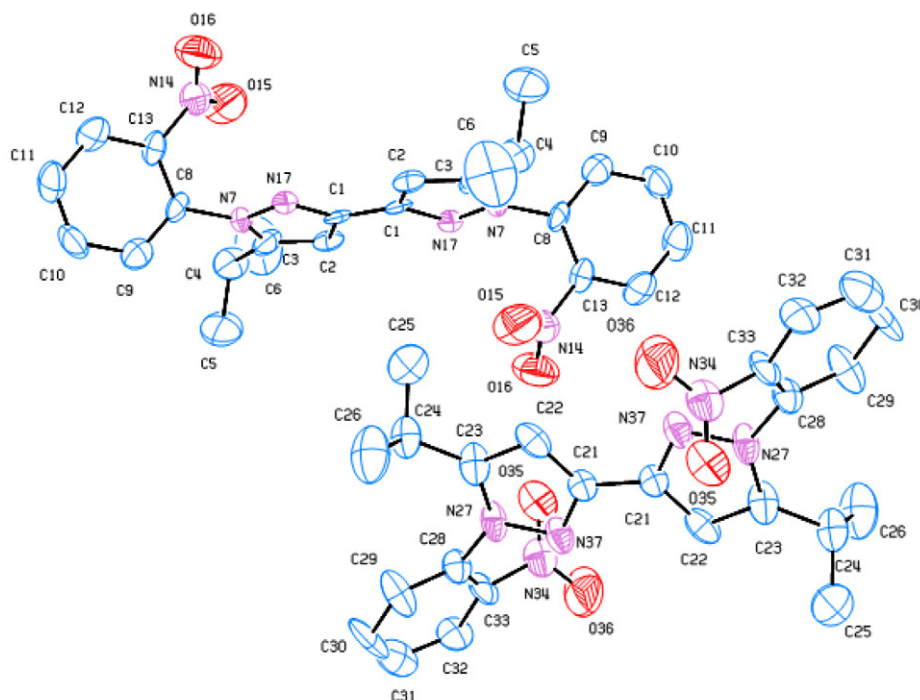


Fig. 2. Representation of the independent molecules of **1**. The H atoms are omitted for clarity.

Nevertheless, some disorder was observed at the isopropyl groups that deviate from the mean plane of the molecule and has been considered in the structural refinements. The compound **5** crystallizes with the tetragonal  $I4_1/a$  symmetry and lattice parameters  $a = b = 11.684(1)$ ,  $c = 19.158(1)$  Å. The unit cell contains 8 molecules, which leads to a calculated density of  $1.109 \text{ g}\cdot\text{cm}^{-3}$ . The eight molecules are symmetry-related and placed on inversion centers lying at the middle of the C1C1 bond as shown in Fig. 3.

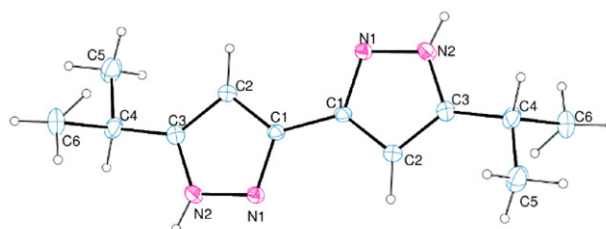


Fig. 3. The molecular unit of **5** with its inversion center in the middle of the C1C1 bond.

The knowledge of this crystal structure was decisive to provide proof of the predominance of the tautomer that the theory predicts with the best stability, i.e. the tautomer having the H positions at N2 atoms.<sup>25</sup>

### 3. 3. Effect of the Substituents on the Molecular Arrangement in the Solid State

The structure of compounds and the crystal morphologies are often strongly related whereas the arrange-

ment of atoms or molecules in the crystal may condition the solid state properties of a compound such as color, solubility, density, stability, reactivity... Good knowledge of the molecular stacking gives advantages in understanding the specific chemical behaviors. Also, having some control over the crystal structures could be a way to modify the properties of a system in the desired direction. Comparison of the crystal structures of bipyrazole derivatives having the same 3,3'-bipyrazole core is a useful source of information on the relationships which may exist between the arrangement of molecules and the presence or the nature of chemical groups R1 and R2.

As it could be seen in **Fig. 4**, the molecules are packed in different ways in the various solid compounds. Nevertheless, some resemblance can be found for compounds **1** and **5** with overlapping of the molecular cores along the a-axis direction.

This could have given rise to  $\pi$ -stacking interactions in these compounds if the molecules had been close enough. In the isomeric compounds **1** and **2**, the molecules only differ by their R2 substituent, either iso- or linear propyl group, yet their molecular packing in the crystal does not show obvious similarities. It is the same between isomeric compounds **1** and **3**, with molecules bearing the same groups R1 and R2 but differing by the fixation of the nitrophenyl group, either in the ortho or para position. Curiously, a certain analogy could be found in the alignment of the molecules that form zig-zag images in the projections along the c-axis in the **2** and **3** isomers (varying both by the nature of R1 and R2 substituents) but also in projection along the a-axis in compound **4**. Even if the three molecules characterizing these compounds have the same isopropyl R2 substituent (like also compound **5**), they are however differentiated by their R1 substituent

changing from o-NO<sub>2</sub>C<sub>6</sub>H<sub>4</sub> in **2** to p-NO<sub>2</sub>C<sub>6</sub>H<sub>4</sub> in **3** and to -CH<sub>2</sub>C<sub>6</sub>H<sub>5</sub> in **4** (it is -H in **5**). Under these conditions, it is extremely difficult to draw conclusions and establish a simple relationship between the geometry of the molecule, the nature and the size of the substituents and a type of molecular packing in the solid state material.

### 3. 4. Effect of the Substituents on the Crystal Parameters

The crystal structures of the compounds **1** and **5** are compared with other solid state structures we previously determined for the bipyrazole derivatives **2-4**.<sup>13,23,24</sup> The main data about these structures are collected in **Table 1**. It is obvious that changing the nature of the R1 and R2 moieties attached to the 3,3'-bipyrazole core of the molecule has great consequences on the crystallographic parameters of the solid compounds. Except in bipyrazole **2**, all the molecules contain an isopropyl group at the R2 position. The crystal symmetry of the solid compounds roughly decreases with the size of the R1 group attached to the nitrogen, from tetragonal in **5** to orthorhombic in **2**, monoclinic in **4** and finally triclinic in **1**. The three isomers **1**, **2** and **3** have rather unlike structures in which both the molecular packing and the symmetry are modified. Note that it is the isomer **2**, with a propyl linear chain at R2 position which displays the highest calculated density. Its unit cell is also twice as large as those of **1** and **3** but contains twice as many molecules.

From **2** to **1**, the replacement of the linear propyl by an isopropyl R2 fragment leads to a less symmetrical arrangement of the molecules ( $P\bar{1}$  instead of P222) and a decrease in the density for the crystal. Conversely, the crystal symmetry evolves from  $P\bar{1}$  to P2<sub>1</sub>/c and the density

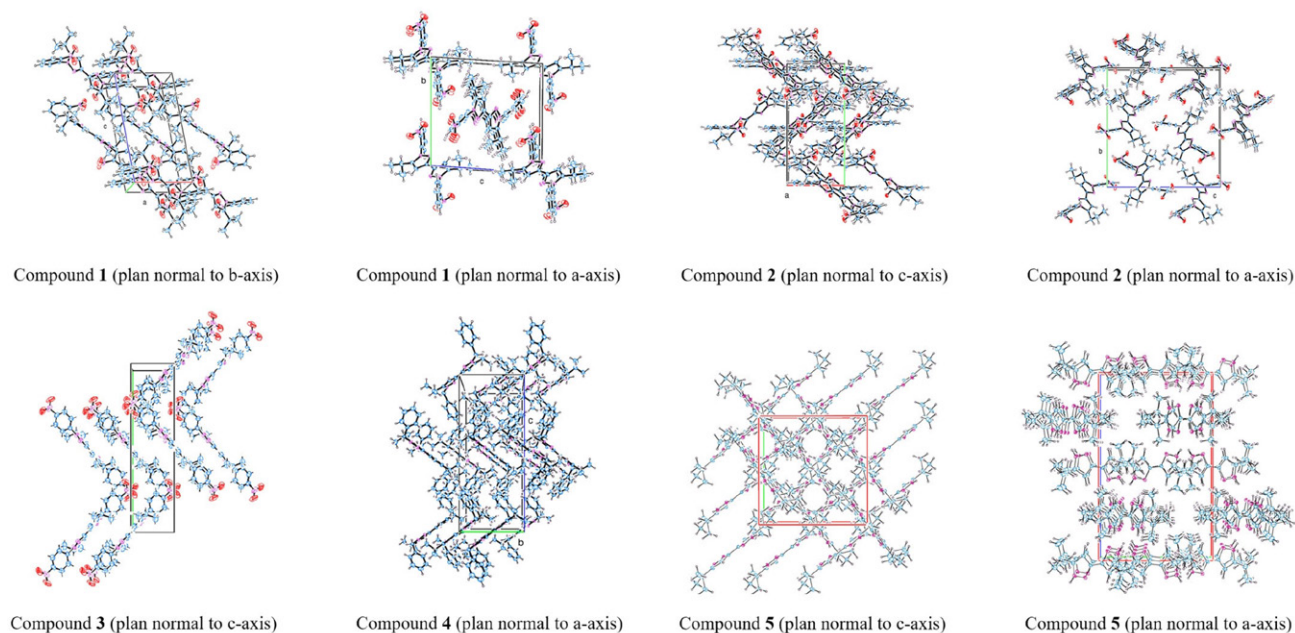


**Fig. 4.** Arrangement of molecules (projections) in the crystal structures for compounds **1-5**

**Table 1.** The main experimental crystal parameters of 3,3'-bipyrzole compounds 1–5

Compound	C <sub>24</sub> H <sub>24</sub> N <sub>6</sub> O <sub>4</sub> 1	C <sub>24</sub> H <sub>24</sub> N <sub>6</sub> O <sub>4</sub> 2	C <sub>24</sub> H <sub>24</sub> N <sub>6</sub> O <sub>4</sub> 3	C <sub>26</sub> H <sub>30</sub> N <sub>4</sub> 4	C <sub>12</sub> H <sub>18</sub> N <sub>4</sub> 5
R1	o-NO <sub>2</sub> C <sub>6</sub> H <sub>4</sub> –	o-NO <sub>2</sub> C <sub>6</sub> H <sub>4</sub> –	p-NO <sub>2</sub> C <sub>6</sub> H <sub>4</sub> –	–CH <sub>2</sub> C <sub>6</sub> H <sub>5</sub> R2	–H
R2	–CH(CH <sub>3</sub> ) <sub>2</sub>	–CH <sub>2</sub> CH <sub>2</sub> CH <sub>3</sub>	–CH(CH <sub>3</sub> ) <sub>2</sub>	–CH(CH <sub>3</sub> ) <sub>2</sub>	–CH(CH <sub>3</sub> ) <sub>2</sub>
M	460.47	460.47	460.47	398.53	218.29
Z	2	4	2	4	8
D (g.cm <sup>–3</sup> )	1.282	1.354	1.327	1.189	1.109
F(000)	484	968	484	856	944
Crystal system	Triclinic	Orthorhombic	Monoclinic	Monoclinic	Tetragonal
Space group	P	P222	P2 <sub>1</sub> /c	P2 <sub>1</sub> /c	I4 <sub>1</sub> /a
a (Å)	7.7113(8)	7.720(1)	6.1760(11)	9.6539(16)	11.6845(13)
b (Å)	12.3926(14)	16.200(2)	23.036(4)	9.7888(17)	11.6845(13)
c (Å)	12.9886(12)	18.058(2)	8.1040(14)	23.562(4)	19.1580(12)
α (°)	92.008(8)	90	90	90	90
β (°)	102.251(8)	90	91.190(15)	90	90
γ (°)	99.655(9)	90	90	90	90
V (Å <sup>3</sup> )	1192.57(31)	2258.5(5)	1152.7(4)	2226.6(6)	2615.6(6)

\*Z represents the number of chemical formula units contained in a unit cell

increases when the R1 nitro-phenyl group fixation changes from ortho in **1** to para in **3**. The bipyrzole compounds **3** and **4** adopt the same crystal symmetry P2<sub>1</sub>/c, yet the nature of the group R1, either nitro-phenyl or benzyl, has consequences on the molecular geometry and it influences the molecular packing that is quite different in the two compounds. The density in **4** is lower than in **3** which leads to less compact stacks for the two molecules which do not contain heteroelement since **5**, with the smallest molecules, has also the lowest density.

### 3. 5. Effect of the Substituents on the Geometry of the Molecules

The geometry of the molecules encountered in the five 3,3'-bipyrzole compounds under study can be characterized using some specific parameters. The selected geometrical parameters such as bond distances, bond angles and torsion angles are schematically represented in Fig. 5.

Their experimental values taken from the X-ray single crystal structures are given in Table 2 with the values measured after geometry optimization without any constraint of isolated molecules. A comparison of these quantities is a way to evaluate both the packing constraints in

the solid and the effects of the nature of R1 and R2 moieties. First of all, it is interesting to note the good correlation between the experimental and theoretical values in each series of parameters selected to describe the geometry of the molecules. Whether in calculations with 6-31G(d,p), 6-311++G(d,p) in Gaussian03W or with DNP and effective core potentials in Dmol<sup>3</sup>, the geometry optimizations lead to very similar results and the correlation coefficients R<sup>2</sup> are mostly higher than 0.985. However, lower values (0.786–0.801) were found for the bond angles in compound **5** which attest to the distortion of the molecule in the crystal. With hydrogen as R1 group, the molecule of **5** is rather small and subjected to greater constraints when it is arranged in the solid state. This is mainly due to the proximity of other molecules with which it is involved in intermolecular interactions. In other cases, the high correlation coefficients confirm a very slight distortion of the bipyrzole core. The main reason is the larger size of the R substituents that hold away the molecules from each other and thus protect the bipyrzole core from deformations by shifting the intermolecular interactions to the molecule periphery.

The resonance effects and ring properties have been discussed for pyrazole compounds<sup>26</sup> and a comparison of the geometrical parameters between pyrazoles and bipyrzoles compounds could also have provided interesting information. This would deserve to be investigated in a future work which could also include effects of neighbouring molecules, as for example fluorinated phenols that may provide infinite supramolecular motifs.<sup>27</sup>

#### 3. 5. 1. Bond Distances

Between the C,C-linked pyrazole rings, the calculated bond distance D1 is always shorter than the experimental distance for the five bipyrzole compounds. Such a

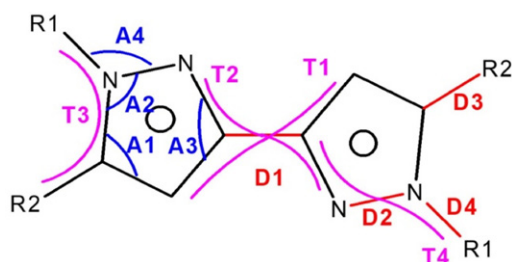


Fig. 5. The parameters selected to describe the geometry of bipyrzole molecules.

Table 2. Experimental and DFT (G03W and Dmol<sup>3</sup>) calculated values for selected geometrical parameters (Å, °) in compounds 1–5

	1			2			3			4			5		
R1	o-NO <sub>2</sub> C <sub>6</sub> H <sub>4</sub> – –CH(CH <sub>3</sub> ) <sub>2</sub>			o-NO <sub>2</sub> C <sub>6</sub> H <sub>4</sub> – –CH <sub>2</sub> CH <sub>2</sub> CH <sub>3</sub>			p-NO <sub>2</sub> C <sub>6</sub> H <sub>4</sub> – –CH(CH <sub>3</sub> ) <sub>2</sub>			–CH <sub>2</sub> C <sub>6</sub> H <sub>5</sub> –CH(CH <sub>3</sub> ) <sub>2</sub>			–H –CH(CH <sub>3</sub> ) <sub>2</sub>		
R2	G03W G03W G03W			G03W G03W G03W			G03W G03W G03W			G03W G03W G03W			G03W G03W G03W		
Method	dmol <sup>3</sup>	dmol <sup>3</sup>	Exp.	dmol <sup>3</sup>	dmol <sup>3</sup>	Exp.	dmol <sup>3</sup>	dmol <sup>3</sup>	Exp.	dmol <sup>3</sup>	dmol <sup>3</sup>	Exp.	dmol <sup>3</sup>	dmol <sup>3</sup>	Exp.
	B3LYP	B3LYP	6-311+G	B3LYP	B3LYP	6-311+G	B3LYP	B3LYP	6-311+G	B3LYP	B3LYP	6-311+G	B3LYP	B3LYP	6-311+G
D1	1.454	1.459	1.458	1.457	1.458	1.458	1.454	1.458	1.458	1.460	1.460	1.461	1.457	1.460	1.468
D2	1.360	1.363	1.361	1.358	1.362	1.367	1.362	1.364	1.362	1.357	1.355	1.375	1.349	1.352	1.323
D3	1.502	1.508	1.507	1.498	1.501	1.479–1.501	1.498	1.501	1.499	1.509	1.507	1.497	1.491	1.496	1.493
D4	1.418	1.418	1.415	1.414	1.414	1.422–1.431	1.414	1.414	1.414	1.416	1.416	1.423	1.440	1.005	1.008
R <sup>2</sup>	0.984	0.983	0.984	0.988	0.985	0.987	0.995	0.994	0.996	0.972	0.972	0.995	0.995	0.998	0.995
A1	105.2	105.4	105.4	105.6	105.5	103.9–105.8	105.6	105.5	105.6	105.8	105.9	106.6	105.4	105.4	109.2
A2	112.7	112.8	112.6	112.5	112.6	114.0–112.3	112.5	112.6	112.5	112.6	112.4	111.7	113.6	113.8	109.4
A3	112.4	111.6	111.4	111.4	111.5	112.1–112.2	111.4	111.5	112.5	111.2	111.0	112.4	111.2	111.4	110.1
A4	117.5	118.0	117.9	118.9	118.1	115.6–118.8	118.9	118.1	118.1	118.5	118.5	117.9	118.9	118.8	124.2
R <sup>2</sup>	0.997	0.992	0.988	0.996	1.000	0.996	0.971	0.950	0.961	0.988	0.984	0.801	0.786	0.801	
T1	179.4	180.0	180.0	177.8	180.0	180.0	178.6	179.9	180.0	172.1	179.8	180.0	172.7	180.0	180.0
T2	179.4	180.0	180.0	176.5	180.0	180.0	179.1	179.8	180.0	174.4	179.8	180.0	176.6	180.0	180.0
T3	1.3	6.3	6.3	3.1	1.6	0.7	0.7	1.2	1.5	3.2	3.5	8.5	1.3	0.2	0.0
T4	178.7	17894	179.0	178.2	177.9	178.3	177.9	178.7	179.0	175.2	176.8	175.6	179.5	180.0	180.0
R <sup>2</sup>	1.000	1.000	1.000	1.000	1.000	1.000	1.000	1.000	1.000	0.999	1.000	1.000	0.999	1.000	1.000

bond lengthening in the crystal is an effect of intermolecular interactions that reduce the electron delocalization on this part of the molecule.

The D2 parameter designates the N–N bond within the pyrazole ring. It has been reported that its length varies over a wide range, from 1.234 to 1.385 Å,<sup>28</sup> with the nature of the substituents bound to the N atoms (here, these are the groups R1). The shortest N–N experimental bond length of 1.323 Å is found in compound 5. The values of 1.369 Å (N7–N17) and 1.367 Å (N27–N37) measured in bipyrzole 1 structure are close to those measured in the isomers 2 (1.363 Å and 1.366 Å) and 3 (1.369 Å). The longer D2 bond of 1.375 Å in 4 indicates a certain reduction in aromaticity compared to compounds 1, 2, 3 in which both D1 and D2 bonds have a more pronounced  $\pi$  character explaining their shortening.

The experimental D3 bond lengths from the isopropyl R2 group to pyrazole ring, of 1.501 Å (C3–C4) and 1.479 Å (C23–C24) in bipyrzole 1 are found slightly shorter than the methyl-phenyl bond of 1.52 Å in toluene.<sup>29</sup> Nevertheless, they do not deviate too much from the D3 distances to isopropyl in 3 (1.493 Å), to propyl in 2 (1.482, 1.493 Å) and from the slightly higher D3 distance of 1.497 Å to benzyl measured in 4.

The D4 links between the group R1 and the N atom of the pyrazole ring have very close length in the three isomers, 1.422–1.431 Å in 1, 1.424–1.426 Å in 2 and 1.423 Å in 3 but they are significantly elongated to 1.440 Å in 4 and even more to 1.493 Å in 5. This reinforces the affirmation made above that the methylene group placed between the pyrazolic and phenyl rings in compound 4 breaks the electron delocalization, which leads to a more covalent and longer D4 bond. When the nitrogen atom is directly bonded to the phenyl ring as in compounds 1–3, the electron delocalization can extend to the phenyl ring and the D4 distance is then shortened.

Besides, according to the literature reports, the C=N bond (adjacent to N–N) in pyrazole compounds ranges from 1.313 to 1.320 Å,<sup>28</sup> which is slightly shorter than the experimental bonds of 1.328 and 1.329 Å in compound 1 and 1.333 Å in compound 5 but also than the calculated bonds ranging from 1.332 to 1.336 in compounds 1–5. It can also be noted that the N–O bond lengths ranging from 1.190 to 1.214 Å in compound 1 are slightly shorter than those from 1.201 to 1.227 Å in isomers 2 and 3.

In summary, the groups R1 and R2 act differently on the geometry of the molecules. The group R1 does not have a very marked effect while the nature of the group R2 greatly influences the bond lengths and the geometry of the bipyrzole core in these C,C-linked pyrazole compounds.

### 3. 5. 2. Bond Angles

The careful examination of experimental angles may provide additional information. The internal C-C-N pyrazolic A1 angle is very close in compounds **2** and **3** (105.5 and 105.7°), it is 103.9 and 105.8° in the two independent molecules of **1**. Instead, it is more obtuse in **4** (106.6°) and in **5** (109.2°) which have not R1 nitrophenyl substituents.

Also, the N-N-C angle, A2, centered on the nitrogen atom outwardly bonded to R1, displays close values in isomers **1** and **2** only differing by their R2 substituent, which leads to claim that the R2 substituent has a very weak influence. Besides, replacing in **1** of the *o*-nitrophenyl R1 group either by a *p*-nitrophenyl (**3**) or by a benzyl (**4**) only causes a small reduction by about 1° of this angle.

On the other hand, the angles A3 or N-C-C centered on the C atom involved in pyrazole rings interconnections measured at 112.1–112.2° in the structure of **1** remain in the order of the A3 angles in other three bipyrazole compounds **1–5**. The A3 angle appears to be independent on the substituents linked to the 3,3'-bipyrazole core.

Finally, values of the C-N-N external pyrazolic A4 angle, 115.6° and 118.8° in the two crystallographically independent molecules of bipyrazole **1**, are quite similar to A4 angles of 118.8 and 118.5° in compound **2**. They lie between the slightly weaker angles of 117.9° in **4** and the markedly higher angles of 124.2 and 129.1° in bipyrazole **5** and **3**, respectively. Of course, only one A4 value is given for the centrosymmetric compounds **3**, **4** and **5** where the molecules are symmetry-related.

### 3. 5. 3. Torsion Angles

Looking first at the torsion angles inside the R1 groups (not reported here) between the nitro groups and the benzyl ring to which they are attached, a difference between isomers **1** and **2** can be noticed. These isomers differing only by the nature of their fragments (linear or branched), these angular values reflect both the steric repulsions between the propyl and nitro groups and the effects of intermolecular interactions. Both their experimental values of 50.3–56.1° in **1**, 48.5–48.9° in **2** and their calculated values of ~38 and 32° in the geometry-optimized isolated molecules give a measure of the amplitude of these effects. This angle of ~1.5° in the optimized molecule of **4** is in agreement with an electronic delocalization on the whole R1 *para* nitrophenyl fragment. Similar changes occur for the pyrazole-to-benzyl torsion angles of 42.3 and 70.2° in crystal of **1**, 48.3 and 70.7° in crystal of **2** while they are ~60° in the optimized isolated molecules of **1** and **2** (and 48° in **3**).

Let's go back now to the specific parameters selected above. The relative position of the two pyrazole rings is characterized by T1 and T2 torsion angles which remain very close to 180° in all the compounds, proving the negligible effect of the R1 and R2 substituents on the bipyrazole core planarity.

The T4 torsion angles are associated with the relative positions of the R1 (at N atom) group and of the pyrazole ring. The comparison of their values in the crystals of **1**, **2** and **3**, where the phenyl ring is directly connected to the pyrazole, shows that this angle varies in the range 176.7–178.9°. The T4 angle is reduced to 175.6° in crystal of **4** where the phenyl ring is linked to pyrazole through a CH<sub>2</sub> group. As stated above, this is linked to the role played by the methylene group with regard to aromaticity.

Finally, as might be expected, the experimental values of T3 angle between R1 and R2 groups indicate that this torsion angle is the most sensitive to the nature of the substituents attached to the pyrazole rings. Switching from a linear to a branched propyl group R2, from **2** to **1**, causes an increase by 1.4° in the T3 angle. By continuing the changes, from **1** to **3**, by fixing the nitro group in the *para* rather than in the *ortho* position, the angle T3 is greatly affected and becomes twice as high (14.6 instead of 6.5°). Instead, from **3** to **4**, replacing the *para*-nitrophenyl group with a benzyl group in **4** gives a decrease down to 8.5° of the T3 angle which thus decreases along the series of investigated bipyrazoles in the order **3** > **4** > **1** > **2**.<sup>13,23,24</sup> As in compound **5**, the group R1 is hydrogen and T3 has a zero value, it is not taken into account in this comparison.

### 3. 6. Effect of Substituents on the Global Reactivity Parameters

The characteristics of the frontier orbitals (HOMO and LUMO) and especially their energy levels are important parameters to understand the behavior of a molecule during a chemical reaction.<sup>29,30</sup> The LUMO will mainly act as an electron acceptor while the HOMO will act as electron donor and the difference in their energy levels represents the stability of the molecule. Measuring the gap ( $E_{\text{HOMO}} - E_{\text{LUMO}}$ ) is therefore a means of evaluating the reactivity of the molecule<sup>31</sup> and the smaller the gap, the greater the chemical reactivity.<sup>32</sup> The ease of polarization of such a molecule induces an increase in the reactivity by the transfer of electrons to an acceptor.<sup>33</sup> To compare the bipyrazole molecules having different R substituents, the energy gaps calculated for the DFT optimized molecules **1–5** are given in **Table 3** with frontier orbital, total and binding energies. The largest gaps are calculated for the lowest reactive molecules of **4** and **5**. Replacing in **4** the benzyl by nitro phenyl groups (fixed either in *ortho* or *para* position) leads to molecules **1** and **3** and increases significantly the reactivity. The energy gap is quite similar for the three isomers **1**, **2** and **3** but shows however a tendency for the isomer **1** to display the lowest values. This indicates a weak sensitivity to the position of the nitro groups attached to the benzyl rings but also to the nature of the alkyl groups linked to the pyrazole rings. Whatever the theory level, the total energy and binding energy are lower for the isomer **3** indicating its better stability.

Table 3. DFT calculated energies (total, binding and frontier orbital) and resulting reactivity indices for molecules 1–5

	1			2			3			4			5		
RI	o-NO <sub>2</sub> C <sub>6</sub> H <sub>4</sub> – –CH(CH <sub>3</sub> ) <sub>2</sub>			o-NO <sub>2</sub> C <sub>6</sub> H <sub>4</sub> – –CH <sub>2</sub> CH <sub>2</sub> C(CH <sub>3</sub> ) <sub>3</sub>			p-NO <sub>2</sub> C <sub>6</sub> H <sub>4</sub> – R2 –CH(CH <sub>3</sub> ) <sub>2</sub>			–CH <sub>2</sub> C <sub>6</sub> H <sub>5</sub> –CH(CH <sub>3</sub> ) <sub>2</sub>			–H –CH(CH <sub>3</sub> ) <sub>2</sub>		
Method	Dmol <sup>3</sup>	G03W	6-31G	Dmol <sup>3</sup>	G03W	6-31G	Dmol <sup>3</sup>	G03W	6-31G	Dmol <sup>3</sup>	G03W	6-31G	Dmol <sup>3</sup>	G03W	6-31G
	B3LYP	6-311++G		B3LYP	6-311++G		B3LYP	6-311++G		B3LYP	6-311++G		B3LYP	6-311++G	
Etot Ha	–1650.63467	–1558.22428	–1558.60332	–1650.63495	–1558.22370	–1558.60432	–1650.65967	–1558.24802	–1558.62493	–1302.99776	–1227.88206	–1228.14922	–561.03455	–529.87299	–529.99958
Ebinding	–107.35615			–107.35643			–107.38115			–89.82212			–36.60678		
Ebinding eV/atom	–50.36743			–50.36756			–50.37916			–40.73643			–45.27827		
HOMO Ha	–0.21776	–0.21114	–0.22490	–0.21867	–0.21206	–0.22513	–0.23451	–0.22729	–0.23964	–0.19235	–0.19867	–0.21090	–0.213422	–0.20445	–0.21923
LUMO Ha	–0.09160	–0.08328	–0.09692	–0.09143	–0.08020	–0.09475	–0.10453	–0.09543	–0.11211	–0.00175	–0.00579	–0.02334	0.004604	0.01197	–0.01216
HOMO ev	–5.93	–5.75	–6.12	–5.95	–5.77	–6.13	–6.38	–6.18	–6.52	–5.23	–5.41	–5.74	–5.81	–5.56	–5.97
LUMO ev	–2.49	–2.27	–2.64	–2.49	–2.18	–2.58	–2.84	–2.60	–3.05	–0.05	–0.16	–0.64	0.13	0.33	–0.33
gap	3.43	3.48	3.48	3.46	3.59	3.55	3.54	3.59	3.47	5.19	5.25	5.10	5.93	5.89	5.63
μM debye	0.00	0.00	0.00	0.77	0.37	0.38	0.00	0.00	0.00	0.01	0.10	0.09	0.01	0.04	0.04
I	5.93	5.75	6.12	5.95	5.77	6.13	6.38	6.18	6.52	5.23	5.41	5.74	5.81	5.56	5.97
A	2.49	2.27	2.64	2.49	2.18	2.58	2.84	2.60	3.05	0.05	0.16	0.64	–0.13	–0.33	0.33
η	1.72	1.74	1.74	1.73	1.79	1.77	1.77	1.79	1.79	2.59	2.62	2.55	2.97	2.94	2.82
μ	–4.21	–4.01	–4.38	–4.22	–3.98	–4.35	–4.61	–4.39	–4.79	–2.64	–2.78	–3.19	–2.84	–2.62	–3.15
χ	4.21	4.01	4.38	4.22	3.98	4.35	4.61	4.39	4.79	2.64	2.78	3.19	2.84	2.62	3.15
σ	0.58	0.57	0.57	0.58	0.56	0.56	0.57	0.56	0.58	0.39	0.38	0.39	0.34	0.34	0.35
ω	5.16	4.61	5.51	5.14	4.41	5.33	6.02	5.37	6.60	1.34	1.47	1.99	1.36	1.16	1.76

The electric dipolar moment  $\mu_M$  can be calculated for the isolated molecules, it measures the separation of positive and negative electric charges within a system. In such molecules having the same substituents on each of the two pyrazole rings, it is not so surprising that no global polarity was calculated for the molecules after geometry optimization. However, the electric dipole moment calculated for the initial geometry (the one in the crystal) that are given in **Table 3** may have a non-zero value, this is the case for the bipyrazole **2** molecule. The orthorhombic symmetry of the crystal structure is such that the atoms of the molecule are not constrained to conform to an inversion center, which leads to a polarity (0.33 to 0.77D depending on the level of theory) reflecting the intermolecular interactions and packing constraints. Contrarily, in molecules of **1**, **3** and **4** the electrons are more equally distributed. The almost-zero (0.04D) dipolar moment in the molecule of **5** suggests that the angular deformations (see above) result rather from the disorder phenomena of the group R2

A series of theoretical indices based on DFT, otherwise known as global reactivity descriptors, are also often used to measure the relative stabilities of isomers and to evaluate the chemical reactivity of molecules. Their values are defined in literature as depending on the ionization energy (I) and electron affinity (A), also related to the energy of the frontier orbitals according to  $I = -E_{\text{HOMO}}$  and  $A = -E_{\text{LUMO}}$ .<sup>25</sup> The electronegativity is  $\chi = (I+A)/2$ , the chemical hardness is  $\eta = (I-A)/2$  and softness  $\sigma = \eta^{-1}$ , the electronic chemical potential  $\mu = -(I+A)/2$  and the global electrophilicity index  $\omega = \mu^2(2\eta)^{-1}$ . These descriptors have been calculated using these relations and their values are reported in **Table 3**.

The deviations in the chemical potential  $\mu$  (and in the electronegativity  $\chi$  of opposite sign) associated with changes in the substituting moieties describe the tendency of gaining electrons towards the molecule.<sup>34</sup> According to the  $\mu$  values calculated (whatever the theoretical level), the molecules are classified in the order  $4 \approx 5 > 2 \approx 1 > 3$ , so that the best acceptor molecules are **4** and **5** while the molecule **3** is that which donates its electrons the most easily. Unlike nitro-phenyl, the benzyl group gives to molecules a greater electron-accepting power. Also, the fixation of the nitro group in position ortho makes the molecule more electron-accepting than its fixation in position para. Based on the molecules examined in this work, the presence of branches on the aliphatic chain in the R2 group decreases the ability of the molecule to accept electrons.

The chemical hardness ( $\eta$ ) is the inverse of chemical softness ( $\sigma$ ) which estimates the capacity of a group of atoms to receive electrons<sup>35</sup> and is directly

linked to the resistance to deformation or to the polarization of the electronic cloud.<sup>36</sup> The values calculated for  $\eta$  lead to divide the molecules studied in two groups: first the isomers **1**, **2** and **3** with low values of chemical hardness ranging from 1.72 to 1.79 eV and secondly, the compounds **4** and **5** with significantly higher values of chemical hardness, 2.55 to 2.97 eV. This means that the benzyl group induces greater resistance to deformation than nitro phenyl. The results are in agreement with what has been reported on the small variations caused by the nature of the R2 alkyl groups and the position (on the phenyl ring) of the nitro groups.<sup>37</sup>

Finally, the global electrophilicity index ( $\omega$ ) gives a measure of the stabilization energy involved in a process during which a molecule acquires an additional electronic charge from its environment.<sup>38</sup> It is interesting to note that a correlation has been established between the electrophilic index and the toxicity<sup>39</sup> and that the organic compounds with the highest electrophilicity indices would be the most toxic. Moreover, it has been stated that the global electrophilicity index provides information about the electrophilic or nucleophilic nature of a medicinal compound.<sup>39</sup> Thus the classification according to the decreasing values of  $\omega$  appears in order **3** > **1** > **2** > **4**  $\approx$  **5** for the molecules of bipyrazole derivatives studied, with very lower indices for the last two compounds, particularly for the molecule **4** comprising a benzyl radical as R1 fragment. With high electrophilicity indices, the molecules of the three isomers **1–3** are characterized with a strong electrophile character.

## 4. Conclusion

The isolated regio-isomer obtained by the N-arylation reaction between 5,5'-diisopropyl-3,3'-bipyrazole and 2-fluoronitrobenzene, adopts the form named 1,1'-bis(2-nitrophenyl)-5,5'-diisopropyl-3,3'-bipyrazole. The nature of the substituents attached to the 3,3'-bipyrazole unit was examined in five bipyrazole derivatives to evaluate their influence both on the molecular structure (geometry of isolated molecule) and on the molecular arrangement in the solid state (crystal structure and molecular interactions). The changes in the crystallographic characteristics (lattice, symmetry...) and in the arrangement of molecules (packing, interactions...) within the crystals are very important. A good correlation is observed between calculated (optimized geometries) and experimental (in the crystal) parameters with regard to the geometric characteristics of the bipyrazole molecules. The global reactivity indices were used to classify the molecules according to their properties and clearly, the molecule with a benzyl substituent stands out from the **3** isomers with a nitrophenyl group.

## Disclosure statement

No potential conflict of interest was reported by the author(s)

## 5. References

1. B. F. Abdel-Wahab, K. M. Dawood, *Arkivoc*, **2012**, i, 491–545. DOI:10.3998/ark.5550190.0013.112
2. H. M. Faidallah, S. A. Rostom, K.A. Khan, *Arch. Pharmacol. Res.* **2015**, 38, 203–215. DOI:10.1007/s12272-014-0392-7
3. I. Bouabdallah, L. A. M'barek, A. Ziad, A. Ramdani, I. Zidane and A. Melhaoui, *Nat. Prod. Res.* **2007**, 21, 298–302. DOI:10.1080/14786410701192801
4. S. Singh, V. Punia, C. Sharma, K. R. Aneja, O. Prakash, R. Pundeer, *J. Heterocycl. Chem.* **2015**, 52, 1817–1822. DOI:10.1002/jhet.1505
5. I. Bouabdallah, I. Zidane, B. Hacht, A. Ramdani, R. Touzani, *J. Mater. Environ. Sci.* **2010**, 1, 20–24.
6. K. Tebbji, A. Aouinti, A. Attayibat, B. Hammouti, H. Oudda, M. Benkaddour, S. Radi, S. Nahle, *Ind. J. Chem. Tech.* **2011**, 18, 244–253.
7. Y. Murakami and T. Yamamoto, *Bull. Chem. Soc. Jpn.* **1999**, 72, 1629–1635. DOI:10.1246/bcsj.72.1629
8. O. Heitaro, I. Takashi, S. Kazuhisa, O. Tetsuo, Bipyrazole derivative, and medicine or reagent comprising the same as active component, US Patent No. 6, 121, 305, date of patent 19 September 2000.
9. I. L. Dalinger, K. Y. Suponitsky, T. K. Shkineva, D. B. Lempert, A. B. Sheremetev, *J. Mater. Chem. A*, **2018**, 6, 14780–14786. DOI:10.1039/C8TA05179H
10. H. Beyzaei, Z. Motraghi, R. Aryan, M. M., Zahedi, A. Samzadeh-Kermani, *Acta Chim. Slov.* **2017**, 64(4), 911–918. DOI:10.17344/acsi.2017.3609
11. E. H. El-Sayed, A. A. Fadda, A. M. El-Saadaney, *Acta Chim. Slov.* **2020**, 67(4), 1024–1034. DOI:10.17344/acsi.2019.5007
12. I. Bouabdallah, R. Touzani, I. Zidane, A. Ramdani, S. Radi, *Arkivoc*, **2006**, xiv, 46–52. DOI:10.3998/ark.5550190.0007.a10
13. I. Bouabdallah, A. Ramdani, I. Zidane, R. Touzani, D. Eddike, S. Radi, A. Haidoux, *J. Mar. Chim. Heterocycl.* **2004**, 3, 39–44.
14. CrysAlis<sup>®</sup>Red 171 software package, Oxford diffraction Ltd, Abingdon, United Kingdom, 2004.
15. G.M. Sheldrick, SHELXS 97. A program for crystal structures solution, University of Göttingen. Germany 1997.
16. G.M. Sheldrick, SHELXL97. A program for refining crystal structures, University of Göttingen. Germany 1997.
17. The Cambridge Crystallographic Data Center (CCDC) <<http://www.ccdc.cam.ac.uk/conts/retrieving.html>>.
18. M. J. Frisch, G. W. Trucks, H. B. Schlegel, G. E. Scuseria, M. A. Robb, J. R. Cheeseman, J. A. Montgomery, Jr., T. Vreven, K. N. Kudin, J. C. Burant, J. M. Millam, S. S. Iyengar, J. Tomasi, V. Barone, B. Mennucci, M. Cossi, G. Scalmani, N. Rega, G. A. Petersson, H. Nakatsuji, M. Hada, M. Ehara, K. Toyota, R. Fukuda, J. Hasegawa, M. Ishida, T. Nakajima, Y. Honda, O. Kitao, H. Nakai, M. Klene, X. Li, J. E. Knox, H. P. Hratchian, J. B. Cross, V. Bakken, C. Adamo, J. Jaramillo, R. Gomperts, R. E. Stratmann, O. Yazyev, A. J. Austin, R. Cammi, C. Pomelli, J. W. Ochterski, P. Y. Ayala, K. Morokuma, G. A. Voth, P. Salvador, J. J. Dannenberg, V. G. Zakrzewski, S. Dapprich, A. D. Daniels, M. C. Strain, O. Farkas, D. K. Malick, A. D. Ra-

- buck, K. Raghavachari, J. B. Foresman, J. V. Ortiz, Q. Cui, A. G. Baboul, S. Clifford, J. Cioslowski, B. B. Stefanov, G. Liu, A. Liashenko, P. Piskorz, I. Komaromi, R. L. Martin, D. J. Fox, T. Keith, M. A. Al-Laham, C. Y. Peng, A. Nanayakkara, M. Challacombe, P. M. W. Gill, B. Johnson, W. Chen, M. W. Wong, C. Gonzalez, J. A. Pople, Gaussian 03, Revision C.02, Gaussian Inc., Pittsburgh, PA, 2003.
19. B. Delley, *J. Chem. Phys.* **1990**, 92, 508–517. DOI:10.1063/1.458452
  20. B. Delley, *Int. J. Quantum Chem.* **1998**, 69, 423–433. DOI:10.1002/(SICI)1097-
  21. T. Keith, J. Millam, GaussView, Version 5, Roy Dennington, Semichem Inc., Shawnee Mission, KS, 2009.
  22. Materials Studio version 3.1.0; Accelrys, Inc., San Diego, 2004.
  23. I. Bouabdallah, A. Ramdani, I. Zidane, D. Eddike, M. Tillard, C. Belin, *Acta Cryst.* **2005**, E61, o4243–o4245. DOI:10.1107/S1600536805037785
  24. I. Bouabdallah, A. Ramdani, I. Zidane, R. Touzani, D. Eddike, A. Haidoux, *J. Mar. Chim. Heterocycl.* **2006**, 5, 52–57. DOI:10.3390/M483
  25. I. Bouabdallah, M. Rahal, T. Harit, A. El Hajbi, F. Malek, D. Eddike, M. Tillard, A. Ramdani, *Chem. Phys. Lett.* **2013**, 588, 208–214. DOI:10.1016/j.cplett.2013.10.046
  26. P. A. Channar, A. Saeed, M. F. Erben, F. A. Larik, S. Riaz, U. Flörke, M. Arshad, *J. Mol. Struct.* **2019**, 1191, 152–157. DOI:10.1016/j.molstruc.2019.04.085
  27. K. V. Domasevitch, *Acta Cryst.* **2008**, C64, o326–o329. DOI:10.1107/S0108270108013632
  28. R. Krishna, D. Velmurugan, R. Murugesan, M. S. Sundaram, R. Raghunathan, *Acta Cryst.* **1999**, C55, 1676–1677.
  29. L.E. Sutton, Tables of interatomic distances and configurations in molecules and ions, The Chemical Society, London, 1965.
  30. M. Ghara, S. Pan, J. Deb, A. Kumar, U. Sarkar, P. K. Chattaraj, *J. Chem. Sci.* **2016**, 10, 1537–1548. DOI:10.1007/s12039-016-1150-9
  31. T. B. Hadda, Z. K. Genc, V. H. Masand, N. Nebbache, I. Warad, S. Jodeh, M. Genc, Y. N. Mabkhot, A. Barakat, H. S. Zamora, *Acta Chim. Slov.* **2015**, 62(3), 679–688.
  32. I. Seghir, N. Nebbache, Y. Meftah, S. E. Hachani, S. Maou, *Acta Chim. Slov.* **2019**, 66(3), 629–637. DOI:10.17344/acsi.2019.5044
  33. D. F. V. Lewis, C. Loannides, D. V. Parke, *Xenobiotica* **1994**, 24, 401–408. DOI:10.3109/00498259409043243
  33. M. A. Migahed, E. G. Zaki, M. M. Shaban, *RSC Adv.* **2016**, 6, 71384–71396. DOI:10.1039/C6RA12835A
  34. D. Pegu, J. Deb, C. Van Alsenoy, U. Sarkar, *Spectrosc. Lett.* **2017**, 50, 232–243. DOI:10.1080/00387010.2017.1308381
  35. P. Senet, P. Chemical, *Chem. Phys. Lett.* **1997**, 275, 527–532. DOI:10.1016/S0009-2614(97)00799-9
  36. D. C. Ghosh, J. Jana, *Current Sci.* **1999**, 76, 570–573. DOI:10.1097/00004032-199905000-00018
  37. I. Bouabdallah, M. Rahal, T. Harit, A. El-hajbi, F. Malek, *J. Mar. Chim. Heterocycl.* **2017**, 16, 124–134.
  38. S. Vinita, S. Pratibha, K. Ashok, *J. Chil. Chem. Soc.* **2014**, 59, 2327–2334. DOI:10.4067/S0717-97072014000100019
  39. R. M. LoPachin, T. Gavin, A. DeCaprio, D. S. Barber, *Chem. Res. Toxicol.* **2012**, 25, 239–251. DOI:10.1021/tx2003257

## Povzetek

Kristalna struktura nove spojine 1,1'-bis(2-nitrofenil)-5,5'-diizopropil-3,3'-bipirazola, **1**, je triklinska tipa  $P\bar{1}$  s sledečimi parametri:  $a = 7.7113(8)$ ,  $b = 12.3926(14)$ ,  $c = 12.9886(12)$  Å,  $\alpha = 92.008(8)$ ,  $\beta = 102.251(8)$ ,  $\gamma = 99.655(9)^\circ$ . Strukturo smo primerjali s tisto za 5,5'-diizopropil-3,3'-bipirazol, **5**, za katerega je bila ugotovljena tetragonalna  $I4_1/a$  struktura s parametri:  $a = b = 11.684(1)$ ,  $c = 19.158(1)$  Å. Primerjavo smo razširili tudi na poprej določene strukture 1,1'-bis(2-nitrofenil)-5,5'-propil-3,3'-bipirazola, **2**, 1,1'-bis(4-nitrofenil)-5,5'-diizopropil-3,3'-bipirazola, **3**, in 1,1'-bis(benzil)-5,5'-diizopropil-3,3'-bipirazola, **4**. Za raziskave molekularnih geometrij in določitve globalnih reaktivnostnih parametrov smo uporabili izračune na osnovi teorije gostotnega funkcionala (DFT). Geometrija izoliranih molekul in ureditev molekul v trdnem stanju smo analizirali glede na naravo skupin, ki so povezane na bipirazolovo jedro.



Except when otherwise noted, articles in this journal are published under the terms and conditions of the Creative Commons Attribution 4.0 International License